D-7-3

Extended Abstracts of the 2015 International Conference on Solid State Devices and Materials, Sapporo, 2015, pp750-751

Catalyst-free growth of $In_xGa_{1-x}As$/InAs coaxial nanorod heterostructures on graphene layers using molecular beam epitaxy

Youngbin Tchoe[1], Janghyun Jo[2], Miyoung Kim[2], and Gyu-Chul Yi[1]

[1] Department of Physics and Astronomy and Research Institute of Advanced Materials,
Seoul National University, Seoul 151-747, Korea
Phone: +82-2-880-2651 E-mail: gcyi@snu.ac.kr
[2] Department of Materials Science and Engineering and Research Institute of Advanced Materials,
Seoul National University, Seoul 151–744, Korea

Abstract

We report the catalyst-free growth of $In_xGa_{1-x}As$/InAs coaxial nanorod heterostructures on large-area graphene layers using molecular beam epitaxy and our investigation of the chemical composition and crystal structure of these heterostructures using electron microscopy. Cross-sectional electron microscopy images showed that $In_xGa_{1-x}As$ layers, having uniform composition, coated heteroepitaxially the entire surface of the InAs nanorods, without interfacial layers or structural defects. The catalyst-free growth mechanism of InAs nanorods on graphene was investigated using in situ reflection high-energy electron diffraction.

1. Introduction

The use of inorganic semiconductors as an active material is desirable for flexible electronic and optoelectronic device applications, due to the many potential advantages over organic semiconductors in terms of lifetime and efficiency [1]. However, continuous, rigid inorganic semiconductor thin films have no tolerance for mechanical deformation. To address this issue, direct growth of semiconductor nanorods on graphene which has high mechanical strength and flexibility was demonstrated recently mainly using metal-organic chemical vapor deposition (MOCVD) [2-4]. Nevertheless, molecular beam epitaxy (MBE) can provide accurate control over the growth parameters for high-quality nanorod heterostructures with very clean and sharp interfaces using various in situ monitoring techniques, such as reflection high electron energy diffraction (RHEED) [5]. Here, we demonstrate the growth of high-quality $In_xGa_{1-x}As$/InAs coaxial nanorod heterostructures on graphene layers using MBE, with a clean interface. Both transmission electron microscopy (TEM) and in situ RHEED were used to investigate the structural properties and growth mechanism of the nanorod heterostructures.

2. Results & Discussions

In this study, we used a two-step MBE process: (i) high-temperature synthesis of ultrafine-core InAs nanorods, and (ii) subsequent low-temperature coating of $In_xGa_{1-x}As$ shell layers on the InAs core nanorods for fabrication of $In_xGa_{1-x}As$/InAs coaxial nanorod heterostructures on graphene layers. The surface morphologies of InAs nanorods and $In_xGa_{1-x}As$/InAs coaxial nanorod heterostructures grown on CVD graphene layers were investigated using scanning electron microscopy (SEM). The mean diameter, height, and density of the InAs nanorods were 70 nm, 10 μm, and 5×10^8 cm^{-2}, respectively. Meanwhile, Figure 1 shows a tilted SEM image of $In_xGa_{1-x}As$/InAs coaxial nanorod heterostructures on CVD graphene layers. After coaxial coating of the $In_xGa_{1-x}As$ shell layer, the mean diameter of nanorods increased to 110 nm, indicating that the average thickness and growth rate of the $In_xGa_{1-x}As$ shell layer was 20 nm and 0.06 Å s^{-1}, respectively. Non-tapered morphology was also observed, indicating that the thickness of the $In_xGa_{1-x}As$ shell layer was uniform over the entire surface.

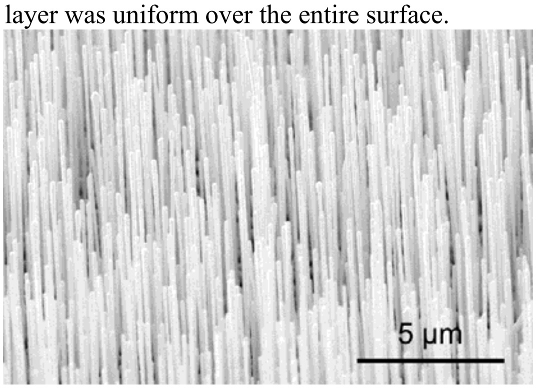

Fig. 1 SEM tilted images of $In_xGa_{1-x}As$/InAs coaxial nanorod heterostructures grown on CVD graphene layers.

MBE-grown InAs nanorods on CVD graphene layers was monitored *in situ* in the initial growth stage using RHEED. Before the nanorod growth, as shown in Fig. 2(a), a streaky RHEED pattern was observed from CVD graphene layers transferred onto a SiO_2/Si substrate. The streaky RHEED patterns of CVD graphene layers remained unchanged, regardless of the azimuthal rotation angles, strongly suggests that the hexagonal graphitic layers were aligned in the (001) direction and the in-plane orientations of each grain were random. When the nanorod growth was initiated (t = 0), the streaky RHEED pattern of CVD graphene layers (Fig. 2(a)) was changed to bright Bragg spots corresponding to InAs nanorods (Fig. 2(b)) within a few seconds of In shutter opening. The appearance of these spots indicated an abrupt change from two-dimensional (2-D) RHEED patterns to three-dimensional (3-D) Bragg diffraction patterns [5].

Additionally, the lattice parameters of the CVD graphene layers and InAs nanorods were estimated by comparing the spacing between the RHEED patterns, as indicated in Figs. 2(a) and (b). The d_{100} interplanar spacing of CVD graphene layers and wurtzite InAs nanorods were 2.1 and 3.7 Å, respectively, which agree with previously reported values [6].

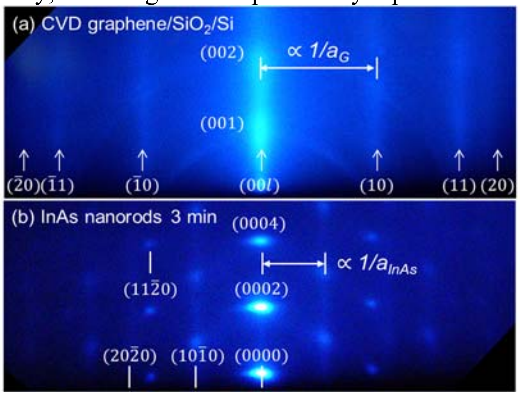

Fig. 2 RHEED patterns during $In_xGa_{1-x}As$/InAs coaxial nanorod heterostructure growth on CVD graphene layers. RHEED patterns of (a) CVD graphene layers transferred onto SiO_2/Si substrates and (b) InAs nanorods grown on CVD graphene layers/SiO_2/Si.

The structural characteristics of $In_xGa_{1-x}As$/InAs coaxial nanorod heterostructures were investigated using TEM. As indicated in the schematic diagram, cross-sectional TEM samples were prepared using FIB. Figure 3(a) shows a cross-sectional BF image of $In_xGa_{1-x}As$/InAs nanorods, exposing the (0001) surface. Since the interface between the $In_xGa_{1-x}As$ and InAs layers was indistinguishable in the BF image without performing chemical analysis, the interface between the $In_xGa_{1-x}As$ shell layer and InAs nanorod core is indicated by dotted hexagonal lines in the figure by comparing STEM image and STEM-EDS mapping results. Both the $In_xGa_{1-x}As$ shell layer and the InAs core exhibited well-developed $\{11\bar{2}0\}$ facets, as opposed to $\{10\bar{1}0\}$ facets, verified exclusively by the fast Fourier transform (FFT) pattern in the inset of Fig. 3(a). This single type of facets were identically observed for ten randomly selected nanorods. Previous TEM studies showed that both $\{10\bar{1}0\}$ and $\{11\bar{2}0\}$ side facets were present in the InAs nanorod system [7]. However, formations of the only $\{11\bar{2}0\}$ facets for $In_xGa_{1-x}As$ shell layer and InAs core may be associated with a smaller surface energy for the $\{11\bar{2}0\}$ side facet than that of the $\{10\bar{1}0\}$ side facet in the InAs nanorod. The epitaxial relationship and atomic structure of $In_xGa_{1-x}As$/InAs coaxial nanorod heterostructures were investigated using HR-TEM [8]. Figure 3(b) shows a HR-TEM image of the region marked with a rectangular box in Fig. 3(a). Significant edge dislocations were not observed at the interface between InAs and $In_xGa_{1-x}As$ layers.

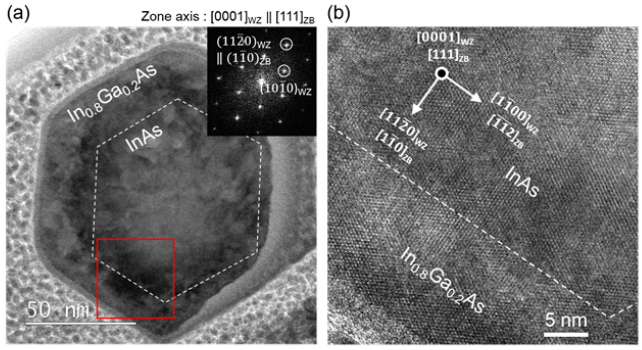

Fig. 3 Microstructure of $In_xGa_{1-x}As$/InAs coaxial nanorod heterostructures on CVD graphene layers. (a) BF-TEM and (b) HR-TEM images of $In_xGa_{1-x}As$/InAs coaxial nanorod heterostructures. The inset diffraction patterns in Fig. 3(a) are obtained via FFT of the HR-TEM images in Fig. 3(b).

3. Conclusions

In conclusion, vertically well-aligned, high-quality $In_xGa_{1-x}As$/InAs coaxial nanorod heterostructures were grown on CVD graphene layers using MBE. From *in situ* RHEED observation, we confirmed that the InAs nanorods grew on CVD graphene layers in a catalyst-free mode. The formation of $In_xGa_{1-x}As$/InAs coaxial nanorod heterostructures was confirmed by STEM and EDS analysis, which showed a clearly defined InAs core and $In_xGa_{1-x}As$ shell layer with uniform composition and thickness. In addition, cross-sectional HR-TEM images demonstrated a clean interface between $In_xGa_{1-x}As$ and InAs. Our work would provide a novel and straightforward pathway for a monolithic integration of semiconductor coaxial nanorod heterostructures on two-dimensional layered materials, which is a key factor to exploit it for flexible electronics and optoelectronics.

Acknowledgements

This work was supported by Seoul National University (SNU)-Yonsei Research Cooperation Program through SNU in 2014. This work was also supported by a grant from CAMP funded by the Ministry of Science and Technology (RIAM), and from the Future-based Technology Development Program (Nano Fields) through the National Research Foundation (NRF) of Korea funded by the Ministry of Education, Science and Technology (MEST) (No. 2014M3A7B4051589, No. 2010-0029325, and NRF 2014023231). Y. Tchoe is grateful for the generous support of the TJ Park Science Fellowship program from the POSCO TJ Park Foundation.

References

[1] G.-C. Yi, *Semiconductor nanostructures for optoelectronic devices*. Springer (2012).
[2] Y.-J. Kim *et al.*, Appl. Phys. Lett. **95**, (2009) 213101.
[3] Y. J. Hong and T. Fukui, ACS nano **5** (2011) 7576-7584.
[4] P. K. Mohseni *et al.*, Nano Lett. **13** (2013) 1153-1161.
[5] S. Hertenberger *et al.*, Appl. Phys. Lett. **98** (2011) 123114.
[6] Y. J. Hong *et al.*, Nano Lett. **12** (2012) 1431-1436.
[7] J. Johansson *et al.*, Nanotechnology **17** (2006) S355.
[8] E. Hilner *et al.*, Nano Lett. **8** (2008) 3978-3982.